---

**Article:**
Gawthrop, P., Wagg, D., Neild, S. et al. (1 more author) (2013) Power-constrained intermittent control. International Journal of Control, 86, (3). 396 - 409. ISSN 0020-7179

https://doi.org/10.1080/00207179.2012.733888

---

*International Journal of Control*
Vol. xx, No. xx, xxx xxxx, 1–24

## RESEARCH ARTICLE

# Power-constrained Intermittent Control

Peter Gawthrop[1], David Wagg[2], Simon Neild[2] and Liuping Wang[3]

[1] Dept. of Electrical and Electronic Engineering,
The University of Melbourne,
VIC 3010, Australia.
e-mail: Peter.Gawthrop@unimelb.edu.au

[2] Department of Mechanical Engineering, University of Bristol, Bristol, BS8 1TR.
e-mail : David.Wagg,Simon.Neild@bristol.ac.uk

[3] Discipline of Electrical Energy and Control Systems, School of Electrical and Computer Engineering,
RMIT University, Melbourne, Victoria 3000, Australia.
e-mail : Liuping.Wang@rmit.edu.au

(*Received 00 Month 200x; final version received 00 Month 200x*)

In this paper input power, as opposed to the usual input amplitude, constraints are introduced in the context of intermittent control. They are shown to result in a combination of quadratic optimisation and quadratic constraints. The main motivation for considering input power constraints is its similarity with semi-active control. Such methods are commonly used to provide damping in mechanical systems and structures. It is shown that semi-active control can be re-expressed and generalised as control with power constraints and can thus be implemented as power-constrained intermittent control. The method is illustrated using simulations of resonant mechanical systems and the constrained nature of the power flow is represented using power-phase-plane plots. We believe the approach we present will be useful for control design of both semi-active and low-power vibration suppression systems.

***Keywords*** Intermittent control; hybrid control; vibration control; semi-active damping; power phase-plane.

ISSN: 0020-7179 print/ISSN 1366-5820 online

DOI: 10.1080/0020717YYxxxxxxxx
http://www.informaworld.com

## 1 Introduction

Model-based predictive control (MPC) (Maciejowski 2002, Wang 2009) combines a quadratic cost function with linear constraints to provide optimal control subject to (hard) constraints on both state and control signal; this combination of quadratic cost and *linear* constraints can be solved using *quadratic programming* (QP) (Fletcher 1987, Boyd and Vandenberghe 2004). The intermittent approach to MPC was introduced (Ronco *et al.* 1999) to reduce on-line computational demand whilst retaining continuous-time like behaviour (Gawthrop and Wang 2007, 2009, Gawthrop *et al.* 2011). This paper considers intermittent control with (hard) constraints on input *power flow*. This combination of quadratic cost and *quadratic* constraints can be solved using *quadratically-constrained quadratic programming* (QCQP) (Boyd and Vandenberghe 2004). Our motivation for this extension of intermittent control in particular, and MPC in general, is the application of intermittent control to semi-active control of vibration.

Semi-active control is an increasingly important control method which is used in a wide range of structural and automotive control applications (Hrovat 1997, Fialho and Balas 2000, Kitching *et al.* 2000, Hong *et al.* 2002, Preumont 2002, Jalili 2002, Sammier *et al.* 2003, Spencer and Nagarajaiah 2003, Verros *et al.* 2005, Shen *et al.* 2006, Giorgetti *et al.* 2006). The method was introduced by Karnopp *et al.* (1974) and involves replacing a conventional actuator by a modulated semi-active element, typically a damper of some type. Such devices are designed to dissipate unwanted vibration energy without adding any additional energy to the system. One of the most popular methods for implementing semi-active control is to use magneto-rheological (MR) dampers (Jansen and Dyke 2000, Yang *et al.* 2004). As a result semi-active devices typically possess the mathematical property of passivity, as defined, for example, by Anderson and Vongpanitlerd (2006). As discussed by Willems (1972), passive systems are a subset of dissipative systems. Because of this passivity constraint, the modulated damper cannot produce any desired force but only those forces which, together with the corresponding power co-variable (relative velocity) satisfy the passivity constraint. Thus, for example, a switching strategy could be used so that the damping coefficient is set to zero when the passivity constraint is violated; this leads to methods such as clipped optimal (Preumont 2002) and hybrid approaches based on intermittent control (Gawthrop *et al.* 2012).

In this paper we will exploit knowledge of existing active controllers to enhance the performance of semi-active controllers. In particular, MPC is a standard design method with well established theoretical properties (Mayne *et al.* 2000). It has been applied to a number of application areas including process control (Qin and Badgwell 2003) and mechanical systems (Giorgetti *et al.* 2006, Cairano *et al.* 2007). Although much implementation and analysis of MPC is conducted

in discrete-time, continuous-time approaches are also possible (Wang 2001, 2009). As mentioned previously, intermittent control provides an alternative approach which combines both continuous and discrete-time aspects; again, some theoretical results are available (Gawthrop 2009, Gawthrop and Wang 2011) and there are applications to mechanical systems (Gawthrop and Wang 2006, 2009, Gawthrop *et al.* 2012) and physiological systems (Gawthrop *et al.* 2011).

Another factor for semi-active control design is the current strong interest in low-energy control. For example, recent results are given by Cassidy *et al.* (2011) and Wang and Inman (2011). This is closely related to the concept of energy harvesting to supply some or all of the semi-active control system power requirements (Nakano *et al.* 2003, Scruggs *et al.* 2007a,b). The concept of "energy harvesting" is closely related to that of "regeneration" (Seth and Flowers 1990, Tucker and Fite 2010).

In contrast to conventional MPC which uses *linear* constraints to satisfy amplitude bounds on control and state amplitude; this paper presents an approach to both semi-active damping and low-energy control by re-expressing the power constraints associated with control signal as *quadratic* optimisation constraints. Together with an intermittent implementation of MPC, this leads to intermittent control with quadratic constraints. Quadratic optimisation with quadratic constraints leads to the QCQP formulation mentioned previously; such problems can be solved using second-order cone programming (Lobo *et al.* 1998).

Bemporad and Morari (1999) show that robust model-predictive control with invariant ellipsoidal terminal sets leads to a QCQP problem. Cannon *et al.* (2001) have shown that the triple-mode model-based predictive control leads to a QCQP problem which can be solved using an active-set method. Soliman *et al.* (2011) show that certain problems in wind-turbine control lead to a QCQP based MPC solution which can be approximated by QP with a polytopic constraint approximation. Quadratic constraints in the context of linear-quadratic optimisation have been considered by Yakubovich (1992) in the infinite horizon case and by Matveev and Yakubovich (1997) in the finite horizon case. However, unlike this paper, they consider constraints based on the *integral* of quadratic functions over time. Quadratic optimisation with quadratic constraints is considered in the context of power flow optimisation by Lavei *et al.* (2011) and in the context of distributed control of positive systems by Rantzer (2011).

The contribution of this paper is to show that designing semi-active control systems using the quadratic constraints approach allows the power flow into and out of the controlled systems to be directly addressed. In addition, we make use of the *power-phase-plane (PPP)* of Seth and Flowers (1990) which gives an immediate qualitative method for assessing the performance of the semi-active controller.

## 2 Unconstrained Intermittent Control

This section contains the background material needed for the rest of the paper; more details and alternative algorithms are presented elsewhere (Gawthrop and Wang 2007, 2009, 2010). As discussed by Gawthrop and Wang (2009), the simple version used here is similar to the "control signal generator" of Åström (2008) and the "model" of Montestruque and Antsaklis (2003).

This paper considers single-input, single-output (SISO) systems given in state space form as:

$$\begin{cases} \frac{d}{dt}\mathbf{x}(t) & = \mathbf{A}\mathbf{x}(t) + \mathbf{B}u(t) + \mathbf{B}_d d(t) \\ y(t) & = \mathbf{C}\mathbf{x}(t) \\ \mathbf{x}(0) & = \mathbf{x}_0 \end{cases} \tag{1}$$

$\mathbf{A}$ is an $n \times n$ matrix, $\mathbf{B}$ and $\mathbf{B}_d$ are $n \times 1$ column vectors and $\mathbf{C}$ is a $1 \times n$ row vector. The $n \times 1$ column vector $\mathbf{x}$ is the system state. The output, control signal and disturbance, $y$, $u$ and $d$ respectively are scalar functions of time and $\mathbf{x}_0$ is the system initial condition. In common with other work relating to semi-active control, it is assumed that the state $\mathbf{x}$ is available.

It is also assumed that there are two power covariables $\mathfrak{u}$ and $\mathfrak{v}$ associated with the control system actuator. For example, in mechanical systems, $\mathfrak{u}$ could be the actuator force and $\mathfrak{v}$ the corresponding relative velocity and in electrical systems $\mathfrak{u}$ could be an applied voltage and $\mathfrak{v}$ the corresponding current. It is assumed that these quantities are linear combinations of the state variables contained in $\mathbf{x}$ and the control signal $u$ and so may be written as:

$$\mathfrak{u} = C_{\mathfrak{u}}\mathbf{x} + D_{\mathfrak{u}}u \tag{2}$$

$$\mathfrak{v} = C_{\mathfrak{v}}\mathbf{x} + D_{\mathfrak{v}}u \tag{3}$$

Specific examples of (2) and (3) appear in Section 4. The linearity assumption of Equations (2) and (3) imposes a restriction on the applicability of the approach of this paper. In the non-linear case, Equations (2) and (3) would represent a linear approximation.

We now consider how the control signal is determined. The *underlying design method* of intermittent control is the conventional continuous-time state-feedback controller with gain $\mathbf{k}$ given by:

$$u(t) = -\mathbf{k}\mathbf{x}(t) \tag{4}$$

However, as seen later, for intermittent control the state vector used is a modified generalised hold vector – see (13). The control signal is generated by considering the undisturbed closed-loop

system:

$$\begin{cases} \frac{d\mathbf{x}_c}{dt}(t) & = \mathbf{A}_c\mathbf{x}_c(t) \\ y(t) & = \mathbf{C}\mathbf{x}_c(t) \\ \mathbf{x}_c(0) & = \mathbf{x}_0 \end{cases} \tag{5}$$

$$\text{where } \mathbf{A}_c = \mathbf{A} - \mathbf{B}\mathbf{k} \tag{6}$$

There are many ways to choose $\mathbf{k}$. One is linear-quadratic regulator (LQR) design (Kwakernaak and Sivan 1972, Goodwin *et al.* 2001) which chooses the control $u$ to minimise the infinite-horizon linear-quadratic cost function:

$$J_{LQR} = \int_0^\infty (\mathbf{x}(t)^T\mathbf{Q}\mathbf{x}(t) + u(t)\mathbf{R}u(t))\,\mathrm{d}t \tag{7}$$

The solution to this optimisation is of the form of (4) where:

$$\mathbf{k} = \mathbf{k}_{LQR} = \mathbf{R}^{-1}\mathbf{B}^T\mathbf{P} \tag{8}$$

and $\mathbf{P}$ is the positive-definite solution of the algebraic Riccati equation (ARE):

$$\mathbf{A}^T\mathbf{P} + \mathbf{P}\mathbf{A} - \mathbf{P}\mathbf{B}\mathbf{R}^{-1}\mathbf{B}^T\mathbf{P} + \mathbf{Q} = 0 \tag{9}$$

Intermittent control makes use of three time frames:

(1) **continuous-time**, over which the controlled system (1) evolves, which is denoted by $t$.

(2) **discrete-time** points at which feedback occurs indexed by $i$. Thus, for example, the discrete-time time instants are denoted $t_i$ and the corresponding system state $\mathbf{x}_i$ is defined as

$$\mathbf{x}_i = \mathbf{x}(t_i) \tag{10}$$

The $i$th intermittent interval is defined as

$$\Delta_i = t_{i+1} - t_i \tag{11}$$

$\Delta_i$ will be assumed to have a constant value of $\Delta_{ol}$ for the rest of this paper.

(3) **intermittent-time** is a continuous-time variable, denoted by $\tau$, restarting at each intermittent interval. Thus, within the $i$th intermittent interval, $\tau = t - t_i$

As discussed by Gawthrop and Wang (2009), in this simple, unconstrained formulation, the

intermittent control signal $\mathbf{U}_i$ is defined at each discrete-time point $t_i$ by:

$$\mathbf{U}_i = \mathbf{x}_i = \mathbf{x}(t_i) \tag{12}$$

where $\mathbf{x}(t_i)$ is the value of $\mathbf{x}(t)$ sampled at time $t = t_i$ corresponding to time $\tau = 0$. Equation (12) does *not* hold in the constrained case considered below. This particular formulation where the hold is initialised to the system state at time $t_i$ is related to both the "control signal generator" of Åström (2008) and the "model" of Montestruque and Antsaklis (2003).

The vector $\mathbf{U}_i$ defines the trajectory generating the inter-sample control signal $u(t)$. In particular, the control signal applied to the system (1), $u(t)$, is generated using the *generalised hold* given by

$$\begin{cases} \frac{d}{d\tau}\mathbf{x}_h(\tau) & = \mathbf{A}_h\mathbf{x}_h(\tau) \\ \mathbf{x}_h(0) & = \mathbf{U}_i \\ u(t_i+\tau) & = -\mathbf{k}\mathbf{x}_h(\tau) \end{cases} \tag{13}$$

where $\mathbf{x}_h$ is the $n$ dimensional state of the generalised hold and $A_h = A_c$ given by (6). The hold state $\mathbf{x}_h$ is initialised to $\mathbf{U}_i$ . An important aim of this paper is to replace the linear intermittent feedback controller (12) by an on-line optimisation procedure so that both state and input hard constraints can be obeyed by the control law. This is considered in Section 3.

## 3 Power-Constrained Intermittent Control

In contrast to the unconstrained case represented by Equation (12), in the constrained case $\mathbf{U}_i \neq \mathbf{x}(t_i)$. It is therefore useful to construct a set of equations describing the evolution of the system state $\mathbf{x}$ and the generalised hold state $\mathbf{x}_h$ that does not rely on equation (12). Following the approach of Gawthrop and Wang (2009), combining (1) and (13) gives such a set of equations:

$$\begin{cases} \frac{d}{d\tau}\mathbf{X}(\tau) & = \mathbf{A}_{xu}\mathbf{X}(\tau) \\ \mathbf{X}(0) & = \mathbf{X}_i \end{cases} \tag{14}$$

where

$$\mathbf{X} = \begin{pmatrix} \mathbf{x} \\ \mathbf{x}_h \end{pmatrix}, \ \mathbf{A}_{xu} = \begin{pmatrix} \mathbf{A} & -\mathbf{B}\mathbf{k} \\ 0_{n\times n} & \mathbf{A}_h \end{pmatrix}, \ \mathbf{X}_i = \begin{pmatrix} \mathbf{x}_i \\ \mathbf{U}_i \end{pmatrix} \tag{15}$$

The differential equation (14) has the explicit solution

$$\mathbf{X}(\tau) = \mathbf{E}(\tau)\mathbf{X}_i \tag{16}$$

$$\text{where } \mathbf{E}(\tau) = e^{\mathbf{A}_{xu}\tau} \tag{17}$$

where $\tau$ is the intermittent continuous-time variable based on $t_i$. Power constraints are based on the system input $\mathfrak{u}$ and the corresponding power covariable $\mathfrak{v}$. To generate the constraints, $\mathfrak{u}$ and $\mathfrak{v}$ must be expressed in terms of the composite state at time $t_i$, $\mathbf{X}_i$. Using equations (2), (3) and (13), it follows that:

$$\mathfrak{u}(\tau) = \gamma_{\mathfrak{u}}\mathbf{E}(\tau)\mathbf{X}_i \tag{18}$$

$$\mathfrak{v}(\tau) = \gamma_{\mathfrak{v}}\mathbf{E}(\tau)\mathbf{X}_i \tag{19}$$

$$\text{where } \gamma_{\mathfrak{u}} = \begin{bmatrix}\mathbf{C}_{\mathfrak{u}} & -D_{\mathfrak{u}}\mathbf{k}\end{bmatrix} \tag{20}$$

$$\text{and } \gamma_{\mathfrak{v}} = \begin{bmatrix}\mathbf{C}_{\mathfrak{v}} & -D_{\mathfrak{v}}\mathbf{k}\end{bmatrix} \tag{21}$$

### 3.1 *Power Constraints*

The vector $\mathbf{X}$, defined in (15), contains the system state and the state of the generalised hold; equation (16) explicitly gives $\mathbf{X}(\tau)$ in terms of the initial value $\mathbf{X}_i$ at time $t_i$.

Hence a constraint on the input power at time $\tau$ can be expressed as:

$$p(\tau) = \mathfrak{u}^T(\tau)\mathfrak{v}(\tau) = \mathbf{X}_i^T\mathbf{\Gamma}_{\mathfrak{u}}(\tau)\mathbf{\Gamma}_{\mathfrak{v}}^T(\tau)\mathbf{X}_i \leq p_{max} \tag{22}$$

$$\text{where } \mathbf{\Gamma}_{\mathfrak{u}} = \gamma_{\mathfrak{u}}\mathbf{E}(\tau) \tag{23}$$

$$\text{and } \mathbf{\Gamma}_{\mathfrak{v}} = \gamma_{\mathfrak{v}}\mathbf{E}(\tau) \tag{24}$$

Following standard MPC practice, constraints beyond the intermittent interval can be included by assuming that the the control strategy will be open-loop in the future; this constraint time horizon is denoted $\tau_c$.

### 3.2 *Optimisation*

Following, for example, Chen and Gawthrop (2006), a modified version of the infinite-horizon LQR cost (7) is used to give a finite horizon expression of the form

$$J_{ic} = \mathbf{x}(\tau_1)^T\mathbf{P}\mathbf{x}(\tau_1) + \int_0^{\tau_1}(\mathbf{x}(\tau)^T\mathbf{Q}\mathbf{x}(\tau) + u(\tau)\mathbf{R}u(\tau))\,\mathrm{d}\tau \tag{25}$$

where the weighting matrices $\mathbf{Q}$ and $\mathbf{R}$ are as used in (7) and $\mathbf{P}$ is the positive-definite solution of the ARE (9). More discussion of this cost function is given by Gawthrop and Wang (2009). We now prove the following Lemma.

**Lemma 3.1** Power-constrained optimisation**:** *The minimisation of the cost function $J_{ic}$ of Equation 25 subject to the constraints* (22) *is equivalent to the solution of the following quadratically-constrained quadratic program (QCQP):*

$$\min_{U_i} \left\{ \mathbf{U}_i^T J_{UU} \mathbf{U}_i + 2\mathbf{x}_i^T J_{Ux} \mathbf{U}_i + \mathbf{x}_i^T J_{xx} \mathbf{x}_i \right\} \tag{26}$$

*subject to* $\max \mathbf{X}_i^T \mathbf{\Gamma}_{\mathfrak{u}}(\tau) \mathbf{\Gamma}_{\mathfrak{v}}^T(\tau) \mathbf{X}_i \leq p_{max}$ *for all* $0 \leq \tau \leq \tau_c$.

*Proof* Using $\mathbf{X}$ from (15), (25) can be rewritten as

$$J_{ic} = \mathbf{X}(\tau_1)^T \mathbf{P}_{xu} \mathbf{X}(\tau_1) + \int_0^{\tau_1} \mathbf{X}(\tau)^T \mathbf{Q}_{xu} \mathbf{X}(\tau)\, d\tau \tag{27}$$

$$\text{where } \mathbf{Q}_{xu} = \begin{pmatrix} \mathbf{Q} & 0_{n\times n} \\ 0_{n\times n} & \mathbf{k}^T \mathbf{R} \mathbf{k} \end{pmatrix} \tag{28}$$

$$\text{and } \mathbf{P}_{xu} = \begin{pmatrix} \mathbf{P} & 0_{n\times n} \\ 0_{n\times n} & 0_{n\times n} \end{pmatrix} \tag{29}$$

Using (16), equation (27) can be rewritten as:

$$J_{ic} = \mathbf{X}_i^T J_{XX} \mathbf{X}_i \tag{30}$$

$$\text{where } J_{XX} = J_1 + e^{\mathbf{A}_{xu}^T \tau_1} \mathbf{P}_{xu} e^{\mathbf{A}_{xu} \tau_1} \tag{31}$$

$$\text{and } J_1 = \int_0^{\tau_1} e^{\mathbf{A}_{xu}^T \tau} \mathbf{Q}_{xu} e^{\mathbf{A}_{xu} \tau}\, d\tau \tag{32}$$

Following Gawthrop and Wang (2009), the $2n \times 2n$ matrix $J_{XX}$ can be partitioned into four $n \times n$ matrices as:

$$J_{XX} = \begin{pmatrix} J_{xx} & J_{xU} \\ J_{Ux} & J_{UU} \end{pmatrix} \tag{33}$$

Using the constraint equation, (22), combining equations (25) – (33) and noting that $J_{XX}$ is symmetrical gives expression (26). □

**Remark 1:** The constraint depends on the current value $\mathbf{X}_i$ of the composite state; from equation (15) it follows that the constraint inequality depends on the current state $\mathbf{x}_i$ as well as the optimised vector $U_i$.

**Remark 2 :** In practice, a finite number, $N_c$, of values of $\tau$ are chosen in the range $0 \leq \tau \leq \tau_c$. These $N_c$ values $\tau_1, \tau_2, \ldots, \tau_i \ldots, \tau_{N_c}$ are then used to precompute $N_c$ vectors $\mathbf{\Gamma}_{\mathfrak{u}i} = \mathbf{\Gamma}_{\mathfrak{u}}(\tau_i)$ and $N_c$ vectors $\mathbf{\Gamma}_{\mathfrak{v}i} = \mathbf{\Gamma}_{\mathfrak{v}}(\tau_i)$.

**Remark 3 :** From equation (12), the unconstrained value of $\mathbf{U}_i$ is $\mathbf{x}_i$. It saves computation if the constraints are checked before optimisation to see if $\mathbf{U}_i = \mathbf{x}_i$ actually satisfies the constraints.

## 4 Examples

The properties of power-constrained intermittent control are illustrated using two examples. The first (Section 4.1) is a simple undamped oscillator which can be taken to represent a unit mass-spring system. The control force $u$ and disturbance force $d$ are collocated. The basic properties are illustrated by the transient response of the system from a non-zero initial condition when the disturbance is zero and by the steady-state response to a sinusoidal disturbance with zero initial conditions. The second (Section 4.2) is a more realistic example of a quarter-car model previously used by Preumont (2002) to compare and contrast vibration control algorithms. Actuator dynamics are also included to illustrate the behaviour when the control signal is not a power covariable. Following Preumont (2002), the behaviour is illustrated by responses to sinusoidal disturbances at various frequencies. The power phase-plane approach of Seth and Flowers (1990) is used to display the results where the power covariables $\mathfrak{u}$ (2) and $\mathfrak{v}$ (3) are plotted against each other thus allowing the effect of power constraints to be easily visualised.

The examples were simulated within GNU octave (Eaton 2002) using the NLopt optimisation algorithms (Johnson 2012). In particular, the COBYLA (Constrained Optimisation by Linear Approximations) algorithm for derivative-free optimisation with nonlinear inequality and equality constraints (Powell 1998) was used. The use of such a general purpose algorithm was justified by the experimental nature of the investigation.

### 4.1 *Simple oscillator*

This example considers the simple harmonic oscillator:

$$\ddot{y}(t) + y(t) = u(t) + d(t) \tag{34}$$

where $y$ is the displacement, $u(t)$ the force control signal and $d(t)$ a disturbance force. This differential equation may be rewritten in the state-space form of (1) where

$$\mathbf{x} = \begin{bmatrix} v \\ y \end{bmatrix}, \ \mathbf{A} = \begin{bmatrix} 0 & -1 \\ 1 & 0 \end{bmatrix}, \ \mathbf{B} = \mathbf{B}_d = \begin{bmatrix} 1 \\ 0 \end{bmatrix}, \ \mathbf{C} = \begin{bmatrix} 0 & 1 \end{bmatrix} \tag{35}$$

and the velocity $v = \dot{y}$. An ideal actuator is assumed and the power covariables are $\mathfrak{u} = u$ and $\mathfrak{v} = v$. It follows that

$$\mathbf{C}_{\mathfrak{u}} = \begin{bmatrix} 0 & 0 \end{bmatrix}, \; D_{\mathfrak{u}} = 1, \; \mathbf{C}_{\mathfrak{v}} = \begin{bmatrix} 1 & 0 \end{bmatrix}, \; D_{\mathfrak{v}} = 0 \tag{36}$$

An unconstrained intermittent controller was designed as in Section 2, equation (7), with the following parameters:

$$\mathbf{Q} = \begin{bmatrix} 0 & 0 \\ 0 & 100 \end{bmatrix}, \; \mathbf{R} = 1 \tag{37}$$

Together with the system parameters of (35), these parameters give:

$$\mathbf{k} = \begin{bmatrix} 4.25 & 9.05 \end{bmatrix}, \; \mathbf{A}_h = \mathbf{A}_c = \begin{bmatrix} -4.25 & -10.05 \\ 1 & 0 \end{bmatrix} \tag{38}$$

This gives closed-loop poles at: $s = -2.13 \pm j2.35$, The open-loop intermittent interval (11) was chosen as $\Delta_i = \Delta_{ol} = 0.01$s.

The power-constrained intermittent control was designed as in Section 3.2 and the effect of the two parameters of Lemma 3.1: $p_{max}$ equation (22) and $\tau_c$ was examined.

Figures 1 and 2 correspond to the transient response of the closed-loop system to an initial condition $\mathbf{x}(0)$

$$\mathbf{x}(0) = \begin{bmatrix} 1 \\ 0 \end{bmatrix} \tag{39}$$

From equation (38), it follows that the initial state in the power phase-plane is:

$$\mathfrak{x} = \begin{bmatrix} \mathfrak{v} \\ \mathfrak{u} \end{bmatrix} = \begin{bmatrix} \mathbf{x}_1(0) \\ -\mathbf{k}\mathbf{x}(0) \end{bmatrix} = \begin{bmatrix} 1 \\ -4.25 \end{bmatrix} \tag{40}$$

In each case, the black line corresponds to the power-constrained intermittent control, the light grey line to the unconstrained intermittent control and the dark grey curves to the power constraints.

Figure 1 corresponds to $p_{max} = 0$; the input power flow must be negative, such that the controller is semi-active, and the constraint boundaries are the axes of the power phase-plane. Figure 1(a)&(b) correspond to a zero constraint horizon $\tau_c = 0$. The unconstrained and power-constrained trajectories are identical until the constraint boundary is reached; from this point, the power-constrained trajectory follows the boundary until the origin is reached when it becomes

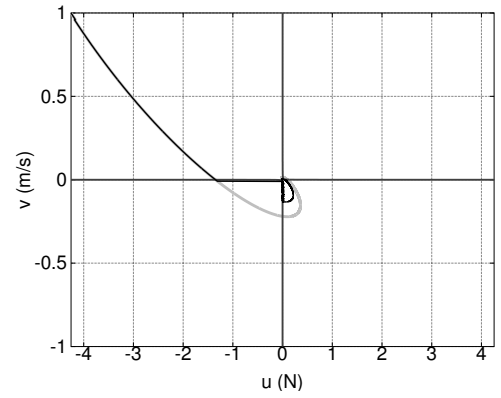


(a) Power phase-plane: $\tau_c = 0$ms

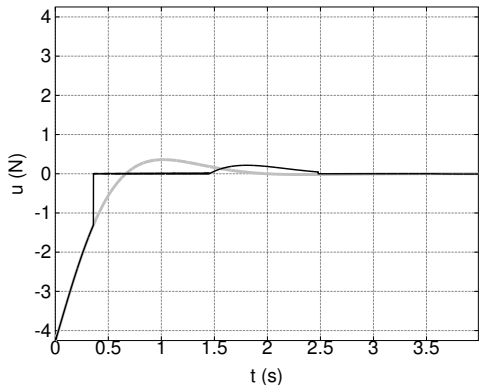


(b) Power covariable $\mathfrak{u}$: $\tau_c = 0$ms

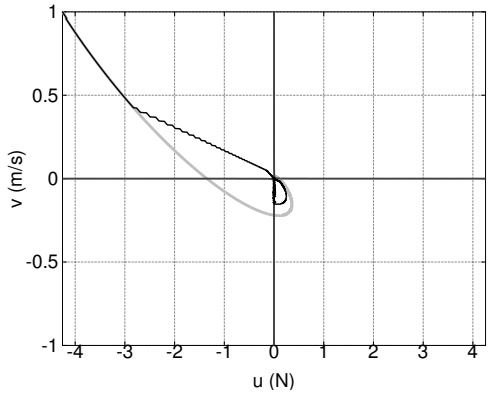


(c) Power phase-plane: $\tau_c = 200$ms

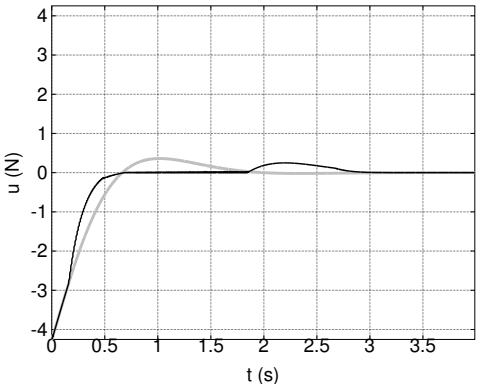


(d) Power covariable $\mathfrak{u}$: $\tau_c = 200$ms

Figure 1. Simple oscillator: transient response with initial condition $v = 1$, $y = 0$ (39), $u = -4.25$ (40) and $p_{max} = 0$. (a) With a zero constraint horizon $\tau_c = 0$, the constrained, active control, trajectory (black) closely follows the unconstrained trajectory (grey) or constraint boundary $p_{max} = 0$ as appropriate. (b) The corresponding control signal $u$ has a corresponding "corner" not exhibited in the unconstrained control. (c) With a non-zero constraint horizon $\tau_c = 200$ms, the constrained trajectory (black) leaves the unconstrained trajectory before the constraint is reached thus anticipating the constraint. (d) The corresponding control signal $u$ is smoother than that of (a)

unconstrained again. The power covariable $\mathfrak{u} = u$ has a discontinuity when the boundary is reached.

To investigate the effect of a non-zero constraint horizon Figure 1(c)&(d) show the effect of a 200ms constraint horizon $\tau_c = 0.2$. The unconstrained and power-constrained trajectories are identical until the constraint boundary is approached; from this point, the power-constrained trajectory diverges from the unconstrained trajectory and gives a smoother approach to the constraint boundary than corresponding to $\tau_c = 0$. The power covariable $\mathfrak{u} = u$ no longer has a discontinuity.

Figure 2 is similar to Figure 1 except that the power constraint is relaxed by setting $p_{max} = 0.01$. The constraint boundaries are now the rectangular hyperbolae shown in Figure 2(a)–(d) but otherwise the behaviour is similar to that described by Figure 1. However, the smoother boundaries do lead to smoother control action as shown by comparing Figures 2(b)&(d) with

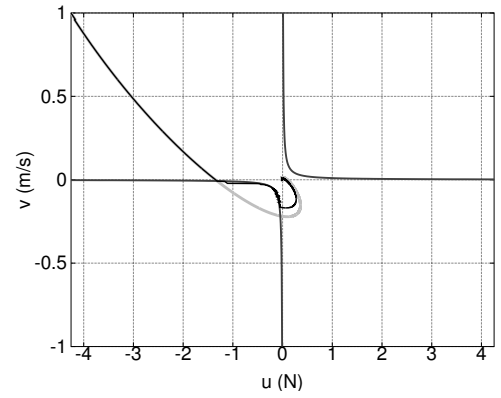


(a) Power phase-plane: $\tau_c = 0$ms

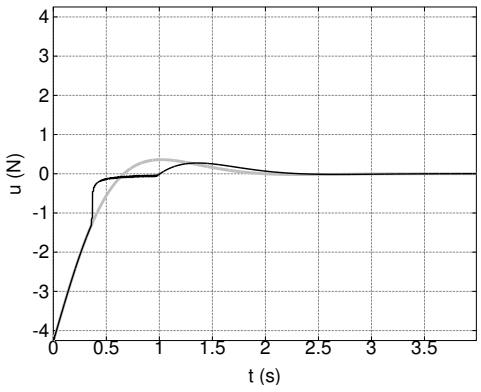


(b) Power covariable $\mathfrak{u}$: $\tau_c = 0$ms

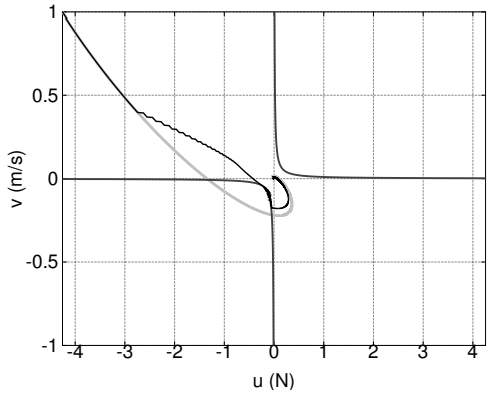


(c) Power phase-plane: $\tau_c = 200$ms

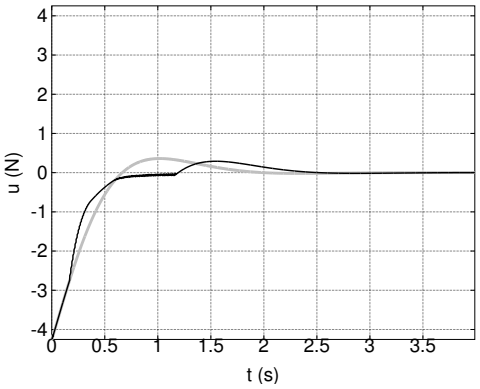


(d) Power covariable $\mathfrak{u}$: $\tau_c = 200$ms

Figure 2. Simple oscillator: transient response with initial condition $v = 1$, $y = 0$ (39), $u = -4.25$ (40) and $p_{max} = 0.01$. In contrast to Figure 1 the non-zero maximum power leads to the hyperbolic constraints leaving the axes around the origin. (a) Again, the constrained trajectory (black) closely follows the unconstrained trajectory (grey) or constraint boundary. (b) The smoother constraint leads to a smoother control signal than that of Figure 1(b). (c) and (d), as in Figure 1 , the non-zero constraint horizon $\tau_c = 200$ms gives smoother control.

Figures 1(b)&(d).

Figures 3&4 correspond to Figures 1&2 except that the initial condition is zero and the disturbance $d$ is a sinusoidal disturbance at the resonant frequency $d = \sin \omega_0 t$ where $w_0 = 1$ rad$s^{-1}$. The figures display two periods after a steady-state has been reached.

Figures 3(a)&(b) show that a zero constraint horizon $\tau_c = 0$ and a zero power constraint $p_{max} = 0$ once again lead to a discontinuous control signal and, once again, this disappears when $\tau_c = 0.2$. Figures 3(a)&(c) also show the increase in the amplitude of the system velocity $v = \mathfrak{v}$ due to the imposition of the power constraints. Figure 4 shows the effect of relaxing the power constraint ($p_{max} = 0.01$) in the sinusoidal disturbance case. The smoother hyperbolic constraint boundaries give a smoother shape to the trajectories and no discontinuities are observed in the control signals shown in Figures 4(b)&(d). Moreover, Figures 4(a)&(c) show that the relaxed constraint reduces the amplitude of the system velocity $v = \mathfrak{v}$ compared to that in Figures

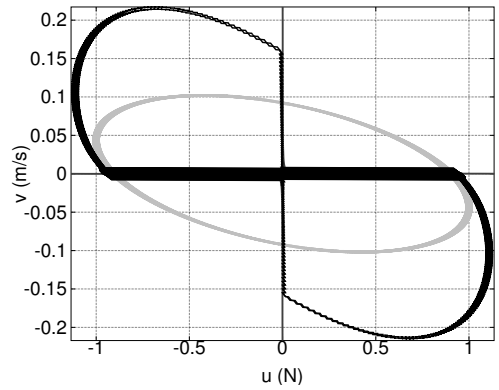


(a) Power phase-plane: $\tau_c = 0$ms

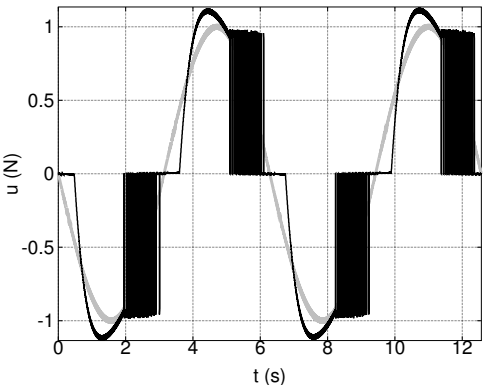


(b) Power covariable u: $\tau_c = 0$ms

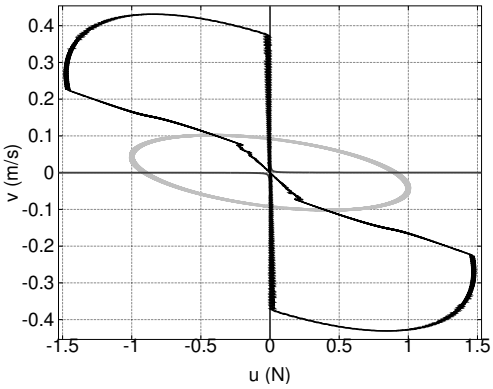


(c) Power phase-plane: $\tau_c = 200$ms

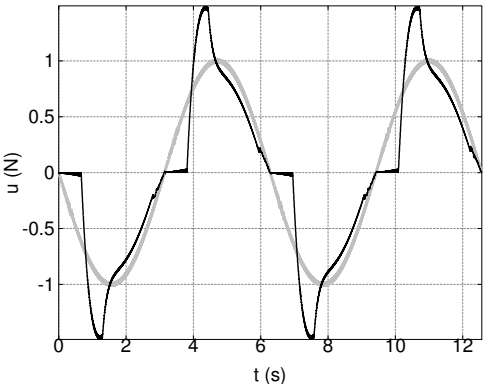


(d) Power covariable u: $\tau_c = 200$ms

Figure 3. Simple oscillator: steady-state sinusoidal response: $p_{max} = 0$. This figure corresponds to Figure 1 but with a sinusoidal disturbance at the resonant frequency $d = \sin 2\pi f_0 t$. (a) With a zero constraint horizon $\tau_c = 0$, the constrained trajectory (black) lies within the negative power quadrants. (b) The corresponding control signal $u$ exhibits a rapid switching, or chattering, phenomenon not exhibited in the unconstrained control. (c) With a non-zero constraint horizon $\tau_c = 200$ms, the constrained trajectory (black) anticipates the constraint. (d) The corresponding control signal $u$ is smoother than that of (a) and does not exhibit chattering. In both cases, the control signal has a small high-frequency component which we attribute to deficiencies in the numerical optimisation.

3(a)&(c).

Each point on the power phase-plane trajectories of Figures 3(a), 3(c), 4(a) and 4(c) corresponds to the instantaneous power $p = uv$ associated with the control signal $u$ and extracted from the system. The corresponding power injected into the system by the disturbance $d$ is $p_0 = dv$ and is thus, through $v$, dependent on the control strategy as well as $d$ itself; this injected power can itself be represented on the power phase-plane. The net power into the system $p_n$, and the corresponding accumulated energy $e_n$ are given by

$$p_n(t) = p(t) + p_0(t) = v(t)[u(t) + d(t)] \tag{41}$$

$$e_n(t) = \int_0^t p_n(t')dt' \tag{42}$$

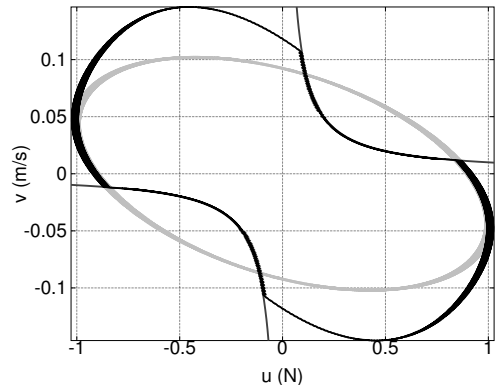


(a) Power phase-plane: $\tau_c = 0$ms

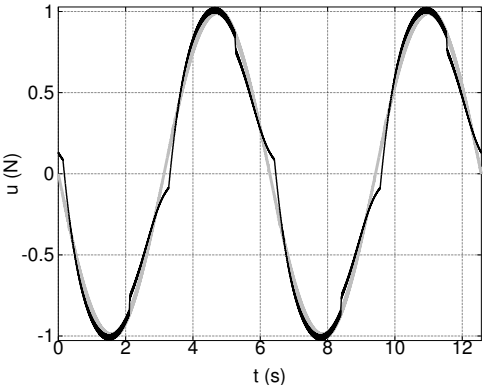


(b) Power covariable u: $\tau_c = 0$ms

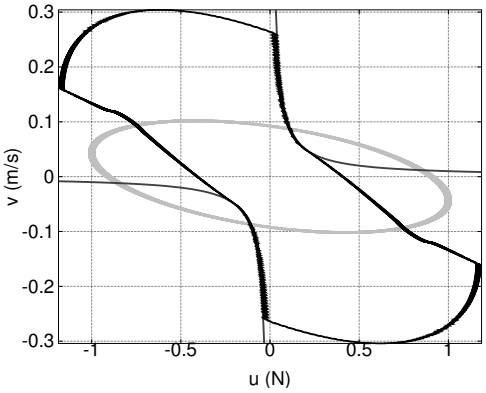


(c) Power phase-plane: $\tau_c = 200$ms

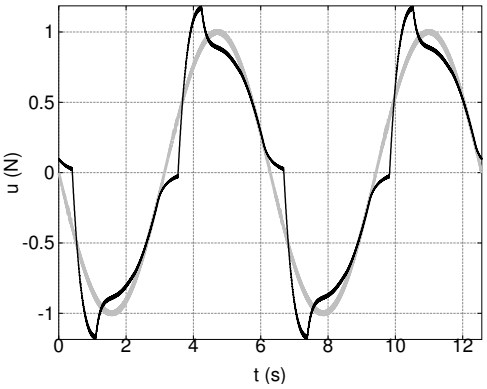


(d) Power covariable u: $\tau_c = 200$ms

Figure 4. Simple oscillator: steady-state sinusoidal response: $p_{max} = 0.01$.This figure corresponds to Figure 2 but with a sinusoidal disturbance at the resonant frequency $d = \sin 2\pi f_0 t$. In contrast to Figure 3 the non-zero maximum power leads to the hyperbolic constraints leaving the axes around the origin. (a) The constrained trajectory (black) closely follows the unconstrained trajectory (grey) or constraint boundary. (b) The smoother constraint leads to a smoother control signal than that of Figure 3(b). (c) and (d) the trajectory no longer follows the constraints so closely.

In this particular example, the system does not, by itself, dissipate energy as there is no damping term in Equation (34). Therefore, in the steady state, the net energy loss in the system over one period must be zero. Figure 5 examines these ideas with reference to the particular example of Figures 3(c) and 3(d) ($p_{max} = 0$, $\tau_c = 200$ms). Figure 5(a) gives the power phase-plane corresponding to $d$ thus the disturbance power $p_0$; it corresponds to Figure 3(c) which shows the control power $p$; as $p_0$ depends on velocity $v$ (Figure 5(b)) it depends on the control strategy as well as the disturbance $d$. Figure 5(c) shows the net power $p_n$ (41) as a function of time $t$ and Figure 5(d) shows the corresponding accumulated energy $e_n$. As predicted, the accumulated energy is zero at the end of each period of the the disturbance $d$. Compared to the example in Figures 3(a) and 3(b) (where $\tau_c = 0$), the velocities are larger and so the power injected by the disturbance and extracted by the controller are larger. Similar results are obtained for the other example conditions of this section.

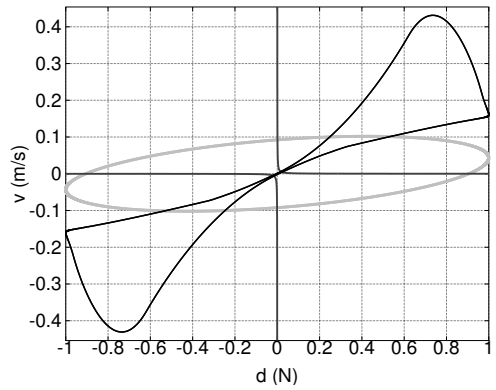


(a) Input power phase-plane

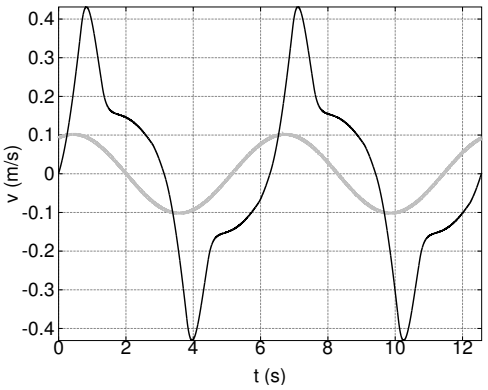


(b) Velocity $v$

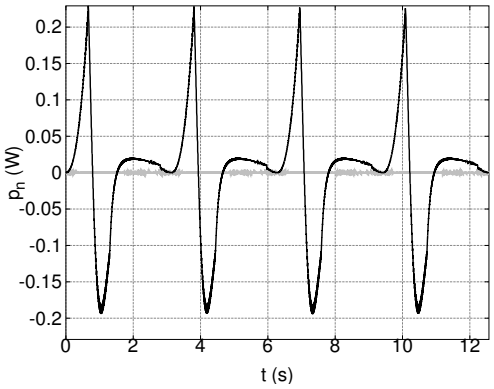


(c) Net power $p_n$

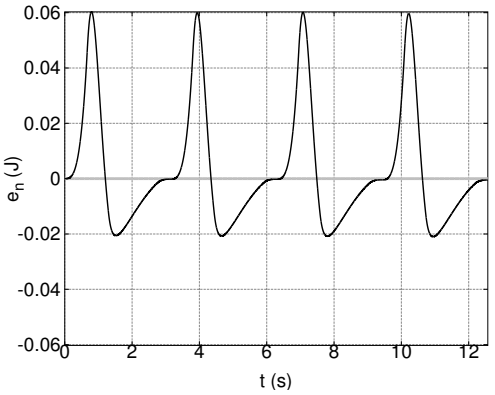


(d) Net energy $e_n$

Figure 5. Power and energy: $p_{max} = 0$, $\tau_c = 200$ms. This Figure corresponds to Figures 3(c) and 3(d); as before, black corresponds to constrained and grey to unconstrained control. (a) shows the power phase-plane corresponding to the disturbance $d$; this lies within the first and third quadrants indicating power inflow. (b) shows the corresponding velocity. (c) Shows the net power flow $p_n = v(u + d)$ into the system when $\tau_c = 0$ corresponding to (d) shows the corresponding accumulated energy $e_n = \int_0^t p_n(t')dt'$. Note that the accumulated energy returns to zero at the end of each period,

### 4.2 *Quarter car model*

The quarter-car model of Figure 6 is used by Preumont (2002) as an example for illustrating passive, active and semi-active vibration control. The same example is used by Gawthrop *et al.* (2012) to illustrate semi-active control based on switched intermittent control.

To make the problem more realistic, and to illustrate the case where the power covariable $\mathfrak{u} \neq u$, the actuator is modelled by the low-pass filter with transfer function $G(s)$ given by

$$G(s) = \frac{1}{1 + 0.01s} \tag{43}$$

The state-space equations are of the form of Equation (1) where $z_3$ is the filter state and:

$$\mathbf{x} = \begin{bmatrix} v_2 & z_2 & v_1 & z_1 & z_3 \end{bmatrix}^T \tag{44}$$

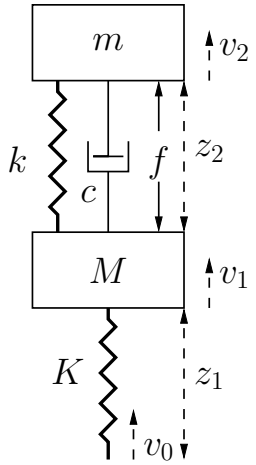


Figure 6. Quarter car model. $m = 240$kg, $M = 36$kg, $k = 16$kN/m, $K = 160$kN/m, $c = 980$Nsec/m. $z_1$ and $z_2$ are the spring extensions in m and $v_1$ and $v_2$ are the mass velocities in m/s. $f$ is an external applied force and $u = -f$ where $u$ is the active control signal.

The matrices $A$, $B$, $B_d$ and $C$ are then given by:

$$\mathbf{A} = \begin{bmatrix} -\frac{c}{m} & -\frac{k}{m} & \frac{c}{m} & 0 & \frac{1}{m} \\ 1 & 0 & -1 & 0 & 0 \\ \frac{c}{M} & \frac{k}{M} & -\frac{c}{M} & -\frac{K}{M} & -\frac{1}{M} \\ 0 & 0 & 1 & 0 & 0 \\ 0 & 0 & 0 & 0 & -100 \end{bmatrix}, \mathbf{B} = \begin{bmatrix} 0 \\ 0 \\ 0 \\ 0 \\ 100 \end{bmatrix}, \mathbf{B}_d = \begin{bmatrix} 0 \\ 0 \\ 0 \\ -1 \\ 0 \end{bmatrix}, \mathbf{C} = \begin{bmatrix} 1 \\ 0 \\ 0 \\ 0 \\ 0 \end{bmatrix}^T \tag{45}$$

In this case, the power covariables are the actuator force $\mathfrak{u} = \zeta$ and velocity $\mathfrak{v} = v_2 - v_1$ hence:

$$\mathbf{C}_u = \begin{bmatrix} 0\,0\,0\,0\,1 \end{bmatrix}, \; D_u = 0, \; \mathbf{C}_v = \begin{bmatrix} 1\,0\,-1\,0\,0 \end{bmatrix}, \; D_v = 0 \tag{46}$$

An unconstrained intermittent controller was designed as in Section 2, equation (7), with the following parameters:

$$\mathbf{Q} = \begin{bmatrix} CC^T \end{bmatrix}, \; \mathbf{R} = 1 \tag{47}$$

Together with the system parameters of (45), these parameters give:

$$\mathbf{k} = \begin{bmatrix} 0.43 & -0.26 & 0.0059 & -1.9 & 0.016 \end{bmatrix} \tag{48}$$

This gives closed-loop poles at: $s = -2.57 \pm j7.42$, $s = -13.92 \pm j67.84$ and $s = -99.91$. The open-loop intermittent interval (11) was chosen as $\Delta_i = \Delta_{ol} = 0.01$s.

The power-constrained intermittent control was designed as in Section 3.2. Figure 7 gives the steady-state response of the system to the disturbance $d = \sin \omega t$ where $\omega = 0.5\omega_0$, $\omega_0$, $2\omega_0$, and $5\omega_0$ and $w_0 = 7.7801$ rads$^{-1}$ is the lower resonant frequency. Figure

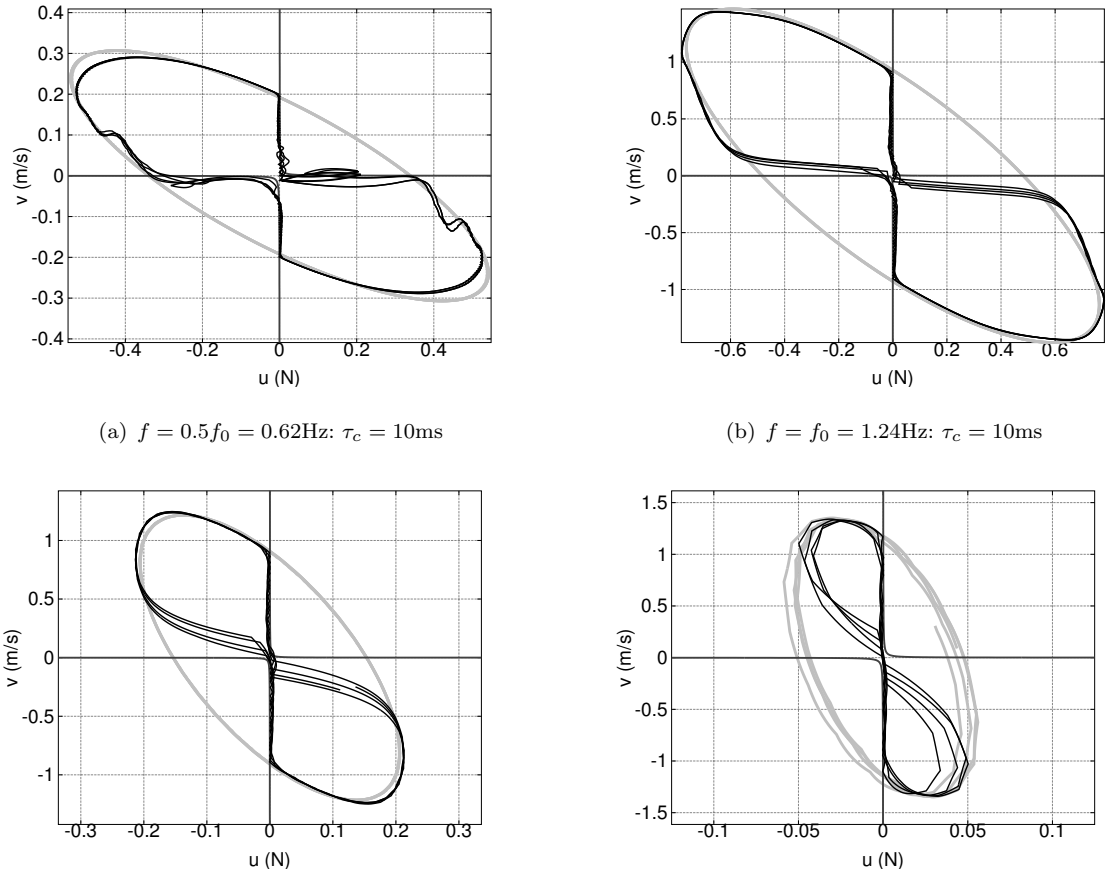


(a) $f = 0.5f_0 = 0.62$Hz: $\tau_c = 10$ms

(b) $f = f_0 = 1.24$Hz: $\tau_c = 10$ms

(c) $f = 2f_0 = 2.48$Hz: $\tau_c = 10$ms

(d) $f = 5f_0 = 6.20$Hz: $\tau_c = 10$ms

Figure 7. Quarter-car model: steady-state sinusoidal response. (a)–(d) give the power-phase plane sinusoidal response at 4 frequencies including the two resonant frequencies. In each case, the constrained trajectory (black) lies within the constraint boundaries (grey hyperbolae) whereas the unconstrained trajectory lies outside the constraints in three of the four cases. The use of a non-zero constraint horizon ($\tau_c = 10$ms) avoids the rapid switching, or chattering, phenomenon associated with zero horizon ($\tau_c = 0$ms) but means that the trajectory does not necessarily follow the constraints closely. The maximum power $p_{max}$ was set to zero.

7(a)–(d) shows the power phase-plane at each of the four frequencies for four periods when the simulation has reached a steady-state. In each case, the power-constrained intermittent controller follows the unconstrained controller when away from constraints and closely follows the constraints when the unconstrained controller violates the constraints. As discussed in Section 4.1, the use of a non-zero constraint horizon of 10ms ($\tau_c = 0.01$) avoids discontinuous control.

There are, however, two discrepancies to be explained. Firstly, the constraints are violated at certain times; this is due to the combination of the disturbance and non-zero intermittent interval $\Delta_{ol}$. The constraint prediction equation (22) assumes $d = 0$ and so the predicted constraint is in error; this effect increases with $\Delta_{ol}$. The effect could be reduced by using a disturbance model within, for example, a disturbance observer. Secondly, the four displayed periods are not identical. This is because the disturbance period is not an integer multiple of the intermittent interval $\Delta_{ol}$ and so the periodic disturbance $d$ does not give a periodic system state $\mathbf{x}$ and so

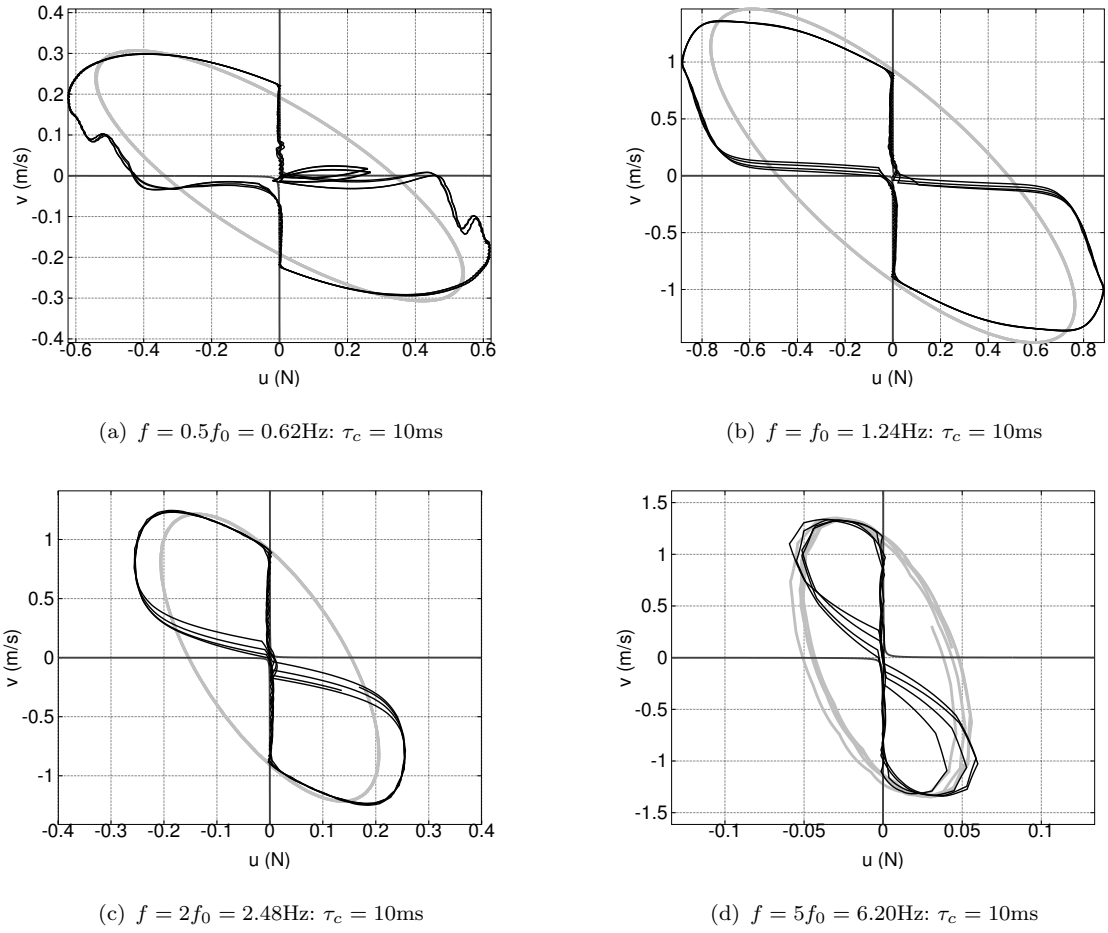


(a) $f = 0.5f_0 = 0.62$Hz: $\tau_c = 10$ms

(b) $f = f_0 = 1.24$Hz: $\tau_c = 10$ms

(c) $f = 2f_0 = 2.48$Hz: $\tau_c = 10$ms

(d) $f = 5f_0 = 6.20$Hz: $\tau_c = 10$ms

Figure 8. Quarter-car model: sensitivity. This figure corresponds to Figure 7 except that the system has been multiplied by a gain of 1.2 (i.e. a 20% increase) without modifying the controller. The control system is robust to this perturbation insofar as the response is not greatly changed by this unmodelled gain.

the phase-plane state $\mathfrak{x}$ is not periodic.

Figure 8 corresponds to Figure 7 except that the system has been multiplied by a gain of 1.2 without modifying the controller to take account of this change. The control system is robust to this perturbation insofar as the response is not greatly changed by this unmodelled gain.

## 5 Conclusion

It has been shown that constraining the power flow into a dynamic system can be implemented using quadratic constraints within a finite-horizon optimisation scheme to give power-constrained intermittent control. Although using a zero-length constraint horizon and a strictly passive limit on the power flow gives clipped-optimal like behaviour, a non-zero constraint horizon gives a smoother anticipatory action. Moreover, relaxing the power limit to allow a small positive power flow similarly gives a smoother control signal. We anticipate that the power-constrained intermittent control approach described here will be useful in applications relating to semi-active

vibration control and low-power control using energy harvesting or regeneration.

A general purpose non-linear optimisation algorithm was used in this work and, although suitable for demonstrating the concepts using simulations, it is neither efficient nor suitable for real-time use. It would be of interest to take advantage of the specific quadratically-constrained quadratic programming (QCQP) form of the optimisation and use the corresponding efficient algorithms (Boyd and Vandenberghe 2004, Lobo *et al.* 1998). The high-frequency component of the control signal visible in Figures 3 and 4 is also believed to be due to deficiencies in the optimisation algorithm. It would therefore be of interest to investigate the exact source of this phenomenon. The example of Section 4.2 illustrated that the method is robust to a quite large change in system gain. Future work will provide a theoretical analysis of robustness to system variation.

As illustrated in Section 4, there are a number of design parameters to be chosen including the constraint horizon $\tau_c$ and the maximum power $p_{max}$. In this paper, these two parameters are chosen in an *ad hoc* manner; future work will formulate design rules for such parameters.

Because the controller constrains the power injected into the system, the resulting constrained controller has passivity properties even if the underlying unconstrained design does not. This is a generalisation of the argument behind semi-active control and will be investigated to give new generalisations of semi-active control.

Constrained control leads to considerations of *feasibility*. This topic has been investigated in the context of model-based predictive control with linear constraints using quadratic programming (Scokaert *et al.* 1999, Mayne *et al.* 2000) and needs to be applied to the QCQP based algorithms discussed here.

The algorithm presented here has a fixed interval $\Delta_i = \Delta_{ol}$. However, as discussed by Gawthrop and Wang (2009a), event-driven versions may be derived. This "control on demand" approach may also have implications for low-energy control and will be further investigated.

The power phase-plane approach of Seth and Flowers (1990) has been shown in Section 4 to provide a useful way of presenting the properties of the method. Future work will consider the power phase-plane approach in more detail including the relation between the power phase-plane of the control signal and that of the disturbance and the relative shapes of the constrained and unconstrained cases.

Although this work was largely motivated by semi-active damping and its implementation using modulated dampers, implementation issues are not discussed in this paper. In particular, when the power constraint (22) is relaxed so that $p_{max} > 0$, the resultant controller can no longer be implemented by a modulated damper. However, future work will investigate whether such a controller could be implemented when the modulated passive controller has energy storage as,

for example, discussed by Potter *et al.* (2011).

This paper has been orientated towards the mechanical engineering application of semi-active vibration control. However, it is applicable to any physical domain, or multiple physical domains, where energy considerations are important.

**Acknowledgements**

Peter Gawthrop is a Visiting Research Fellow at the University of Bristol. He is also partially supported by the linked EPSRC Grants EP/F068514/1, EP/F069022/1 and EP/F06974X/1 "Intermittent control of man and machine" and gratefully acknowledges the many discussions about intermittent control with Henrik Gollee, Ian Loram and Martin Lakie. The authors wish to thank Irina Lazar, University of Bristol, for her constructive comments on the draft of this paper.

The authors gratefully acknowledge the many insightful comments of the referees which have lead to an improved paper.

**References**

Anderson, B.D.O., and Vongpanitlerd, S., *Network Analysis and Synthesis: A Modern Systems Theory Approach*, First published 1973 by Prentice-Hall, Dover (2006).

Åström , K.J. (2008), "Event Based Control," in *Analysis and Design of Nonlinear Control Systems* eds. A. Astolfi and L. Marconi, Heidelberg: Springer, pp. 127–147.

Bemporad, A., and Morari, M. (1999), "Robust model predictive control: A survey," (Vol. 245, eds. A. Garulli and A. Tesi, Springer, pp. 207–226.

Boyd, S., and Vandenberghe, L., *Convex optimization*, Cambridge Univ Press (2004).

Cairano, S.D., Bemporad, A., Kolmanovsky, I.V., and Hrovat, D. (2007), "Model predictive control of magnetically actuated mass spring dampers for automotive applications," *International Journal of Control*, 80, 1701–1716.

Cannon, M., Kouvaritakis, B., and Rossiter, J. (2001), "Efficient active set optimization in triple mode MPC," *Automatic Control, IEEE Transactions on*, 46, 1307 –1312.

Cassidy, I.L., Scruggs, J.T., and Behrens, S. (2011), "Optimization of partial-state feedback for vibratory energy harvesters subjected to broadband stochastic disturbances," *Smart Materials and Structures*, 20, 085019.

Chen, W.H., and Gawthrop, P.J. (2006), "Constrained predictive pole-placement control with linear models," *Automatica*, 42, 613–618.

Eaton, J.W., *GNU Octave Manual*, Bristol: Network Theory Limited (2002).

Fialho, I.J., and Balas, G.J. (2000), "Design of nonlinear controllers for active vehicle suspensions using parameter-varying control synthesis," *Vehicle System Dynamics*, 33, 351–370.

Fletcher, R., *Practical Methods of Optimization. 2nd Edition*, Chichester: Wiley (1987).

Gawthrop, P., Loram, I., Lakie, M., and Gollee, H. (2011), "Intermittent Control: A Computational Theory of Human Control," *Biological Cybernetics*, 104, 31–51.

Gawthrop, P., and Wang, L. (2011), "The system-matched hold and the intermittent control separation principle," *International Journal of Control*, 84, 1965–1974.

Gawthrop, P.J. (2009), "Frequency Domain Analysis of Intermittent Control," *Proceedings of the Institution of Mechanical Engineers Pt. I: Journal of Systems and Control Engineering*, 223, 591–603.

Gawthrop, P.J., Neild, S.A., and Wagg, D.J. (2012), "Semi-active damping using a hybrid control approach," *Journal of Intelligent Material Systems and Structures*, Published online February 21, 2012.

Gawthrop, P.J., and Wang, L. (2006), "Intermittent predictive control of an inverted pendulum," *Control Engineering Practice*, 14, 1347–1356.

Gawthrop, P.J., and Wang, L. (2007), "Intermittent Model Predictive Control," *Proceedings of the Institution of Mechanical Engineers Pt. I: Journal of Systems and Control Engineering*, 221, 1007–1018.

Gawthrop, P.J., and Wang, L. (2009), "Constrained intermittent model predictive control," *International Journal of Control*, 82, 1138–1147.

Gawthrop, P.J., and Wang, L. (2009a), "Event-driven Intermittent Control," *International Journal of Control*, 82, 2235 – 2248.

Gawthrop, P.J., and Wang, L. (2010), "Intermittent redesign of continuous controllers," *International Journal of Control*, 83, 1581–1594.

Giorgetti, N., Bemporad, A., Tseng, H.E., and Hrovat, D. (2006), "Hybrid model predictive control application towards optimal semi-active suspension," *International Journal of Control*, 79, 521–533.

Goodwin, G., Graebe, S., and Salgado, M., *Control System Design*, New Jersey: Prentice Hall (2001).

Hong, K.S., Sohn, H.C., and Hedrick, J.K. (2002), "Modified skyhook control of semi-active suspensions: A new model, gain scheduling, and hardware-in-the-loop tuning," *Journal of Dynamic Systems Measurement and Control-Transactions of the ASME*, 124, 158–167.

Hrovat, D. (1997), "Survey of advanced suspension developments and related optimal control applications," *Automatica*, 33, 1781–1817.

Jalili, N. (2002), "A comparative study and analysis of semi-active vibration-control systems," *Journal of Vibration & Acoustics-Transactions of the ASME*, 124, 593–605.

Jansen, L.M., and Dyke, S.J. (2000), "Semiactive control strategies for MR dampers: Comparative study," *Journal of Engineering Mechanics—ASCE*, 126, 795–803.

Johnson, S.G., *The NLopt nonlinear-optimization package*, MIT, http://ab-initio.mit.edu/nlopt (2012).

Karnopp, D., Crosby, M., and Harwood, R. (1974), "Vibration control using semi-active force generators," *ASME Journal of Engineering for Industry*, 96, 619–626.

Kitching, K.J., Cole, D.J., and Cebon, D. (2000), "Performance of a semi-active damper for heavy vehicles," *Journal of Dynamic Systems Measurement & Control—Transactions of the ASME*, 122, 498–506.

Kwakernaak, H., and Sivan, R., *Linear Optimal Control Systems*, New York: Wiley (1972).

Lavei, J., Rantzer, A., and Low, S. (2011), "Power flow optimization using positive quadratic programming?," in *Proc. 18th IFAC World Congress*, Milano, August.

Lobo, M.S., Vandenberghe, L., Boyd, S., and Lebret, H. (1998), "Applications of second-order cone programming," *Linear Algebra and its Applications*, 284, 193 – 228.

Maciejowski, J., *Predictive Control with Constraints*, Prentice Hall (2002).

Matveev, A., and Yakubovich, V. (1997), "Nonconvex Problems of Global Optimization: Linear-Quadratic Control Problems with Quadratic Constraints," *Dynamics and Control*, 7, 99–134.

Mayne, D., Rawlings, J., Rao, C., and Scokaert, P. (2000), "Constrained model predictive control: Stability and optimality," *Automatica*, 36, 789–814.

Montestruque, L.A., and Antsaklis, P.J. (2003), "On the model-based control of networked systems," *Automatica*, 39, 1837 – 1843.

Nakano, K., Suda, Y., and Nakadai, S. (2003), "Self-powered active vibration control using a single electric actuator," *Journal of Sound and Vibration*, 260, 213 – 235.

Potter, J.N., Neild, S.A., and Wagg, D.J. (2011), "Quasi-active suspension design using magnetorheological dampers," *Journal of Sound and Vibration*, 330, 2201 – 2219, Dynamics of Vibro-Impact Systems.

Powell, M.J.D. (1998), "Direct search algorithms for optimization calculations," *Acta Numerica*, 7, 287–336.

Preumont, A., *Vibration control of active structures: an introduction*, 2nd ed., Vol. 96 of *Solid Mechanics and its Applications*, Dordrecht: Kluwer (2002).

Qin, S.J., and Badgwell, T.A. (2003), "A survey of industrial model predictive control technology," *Control Engineering Practice*, 11, 733 – 764.

Rantzer, A. (2011), "Distributed control using positive quadratic programming," in *Control Conference (CCC), 2011 30th Chinese*, Hefei, july, pp. 1 –4.

Ronco, E., Arsan, T., and Gawthrop, P.J. (1999), "Open-Loop Intermittent Feedback Control: Practical Continuous-time GPC," *IEE Proceedings Part D: Control Theory and Applications*, 146, 426–434.

Sammier, D., Sename, O., and Dugard, L. (2003), "Skyhook and H-infinity control of semi-active suspensions: Some practical aspects," *Vehicle System Dynamics*, 39, 279–308.

Scokaert, P.O.M., Mayne, D.Q., and Rawings, J.B. (1999), "Suboptimal model predictive control (feasibility implies stability)," *IEEE Trans. on Automatic Control*, 44, 648–654.

Scruggs, J.T., Taflanidis, A.A., and Iwan, W.D. (2007a), "Non-linear stochastic controllers for semiactive and regenerative systems with guaranteed quadratic performance boundsPart 1: State feedback control," *Structural Control and Health Monitoring*, 14, 1101–1120.

Scruggs, J.T., Taflanidis, A.A., and Iwan, W.D. (2007b), "Non-linear stochastic controllers for semiactive and regenerative systems with guaranteed quadratic performance boundsPart 2: Output feedback control," *Structural Control and Health Monitoring*, 14, 1121–1137.

Seth, B., and Flowers, W.C. (1990), "Generalized Actuator Concept for the Study of the Efficiency of Energetic Systems," *Journal of Dynamic Systems, Measurement, and Control*, 112,

233–238.

Shen, Y., Golnaraghi, M.F., and Heppler, G.R. (2006), "Semi-active vibration control schemes for suspension systems using magnetorheological dampers," *Journal of Vibration & Control*, 12, 3–24.

Soliman, M., Malik, O., and Westwick, D. (2011), "Ensuring Fault Ride Through for Wind Turbines with Doubly Fed Induction Generator: a Model Predictive Control Approach," in *18th IFAC World Congress*, Milan, pp. 1710–1715.

Spencer, B.F., and Nagarajaiah, S. (2003), "State of the art of structural control," *Journal of Structural Engineering-ASCE*, 129, 845–856.

Tucker, M., and Fite, K. (2010), "Mechanical damping with electrical regeneration for a powered transfemoral prosthesis," in *Advanced Intelligent Mechatronics (AIM), 2010 IEEE/ASME International Conference on*, Montreal, ON, july, pp. 13 –18.

Verros, G., Natsiavas, S., and Papadimitriou, C. (2005), "Design optimization of quarter-car models with passive and semi-active suspensions under random road excitation," *Journal of Vibration & Control*, 11, 581–606.

Wang, L. (2001), "Continuous Time Model Predictive Control Using Orthonormal Functions," *Int. J. Control*, 74, 1588–1600.

Wang, L., *Model Predictive Control System Design and Implementation Using MATLAB*, 1st ed., Springer (2009).

Wang, Y., and Inman, D.J. (2011), "Comparison of Control Laws for Vibration Suppression Based on Energy Consumption," *Journal of Intelligent Material Systems and Structures*, 22, 795–809.

Willems, J.C. (1972), "Dissipative Dynamical Systems, Part I: General Theory, Part II: Linear System with Quadratic Supply Rates," *Arch. Rational Mechanics and Analysis*, 45, 321–392.

Yakubovich, V.A. (1992), "Nonconvex optimization problem: The infinite-horizon linear-quadratic control problem with quadratic constraints," *Systems and Control Letters*, 19, 13 – 22.

Yang, G.Q., Spencer, B.F., Jung, H.J., and Carlson, J.D. (2004), "Dynamic modeling of large-scale magnetorheological damper systems for civil engineering applications," *Journal of Engineering Mechanics-ASCE*, 130, 1107–1114.